Front. Chem. China 2009, 4(1): 48–51
DOI 10.1007/s11458-009-0007-x

RESEARCH ARTICLE

Shumin HAN, Yuan LI, Zhong ZHANG, Xilin ZHU, Jinhua LI, Lin HU

Structural and electrochemical properties of high-capacity Ml-Mg-Ni-based hydrogen storage alloys

Abstract The Ml-Mg-Ni-based (Ml = La-rich mixed lanthanide) hydrogen storage alloy $Ml_{0.88}Mg_{0.12}Ni_{3.0}Mn_{0.10}Co_{0.55}Al_{0.10}$ was prepared by inductive melting. The micro-structure was analyzed by XRD and SEM. The alloy consists mainly of $CaCu_5$-type phase, Ce_2Ni_7-type phase and Pr_5Co_{19}-type phase. The electrochemical measurements show that the maximum discharge capacity is 386 mAh/g, 16.3% higher than that of the commercial AB_5-type alloy (332 mAh/g). At discharge current density of 1 100 mA/g, high rate dischargeability is 62%, while that of the AB_5-type alloy is only 45%. The discharge capacity decreases to 315 mAh/g after 300 charge/ discharge cycles, 81.5% of the maximum discharge capacity.

Keywords Ni/MH batteries, hydrogen storage alloys, Ml-Mg-Ni-based alloys, electrochemical properties

Nickel/metal hydride (Ni/MH) batteries using hydrogen storage alloys as negative electrode materials are a new type of secondary batteries with many advantages, such as high energy density, durability to over-charge/discharge and environmental friendliness, so they are widely used in portable electronic instruments. The commercial AB_5-type alloys are easily activated and have a long cycle life, however, their capacities are comparatively lower due to restrictions from their single-phase structure (The theoretical electrochemical capacity of $LaNi_5$ is only 370 mAh/g) [1]. Furthermore, the available capacity (310–330 mAh/g) of these alloys has gotten closer to their limits via improvements through several years, thus showing lesser potential for promotion. The situation mentioned above is a barrier for further development of Ni/MH batteries, so it is urgent to find new types of hydrogen storage alloys with higher capacity. In recent years, Kadir *et al*. [2,3] have prepared a new type of alloy with a general formula of RMg_2Ni_9 (R = rare earths, Ca or Y), and the hydrogen capacity of these alloys reach 1.8–1.87 (wt)% (weigh percent). Kohno *et al*. [4] investigated electrochemical properties of the $La_{0.7}Mg_{0.3}Ni_{2.8}Co_{0.5}$ alloy, finding that capacity was as high as 410 mAh/g, with good stability within 30 cycles. Thus, the La-Mg-Ni-based hydrogen storage alloys with $PuNi_3$-type structure are considered as promising candidates for negative electrode materials of Ni/MH batteries. Akiba *et al*. [5] reported a superlattice structure for this type of alloys-stacking of AB_2 sub-slabs and AB_5 sub-slabs. Most of the recent work has been focused on B-site metals, reporting effects of Ni, Mn, Co and Al on electrochemical properties of the alloys, and it has been found that the appropriate content of these elements is beneficial to the alloys' electrochemical properties [6–10]. However, some constituent elements, such as La and Mg, are subject to serious corrosion from the alkaline electrolyte, leading to a rapid decrease in capacity. Our previous work showed that substitution of La-rich mixed lanthanide for a pure La and B-site multi-component are helpful in improving cycling stability [11,12].

1 Experimental

1.1 Alloy preparation

The $Ml_{0.88}Mg_{0.12}Ni_{3.0}Mn_{0.10}Co_{0.55}Al_{0.10}$ alloy was prepared by inductive melting La-rich mixed lanthanide Ml (Ml consists of 71.6%La, 19.7%Ce, 1.9%Pr, 6.3%Nd and 0.5% impurity), Ni, Co, Mn, Al and Mg-Ni under an argon atmosphere. In order to reduce Mg loss resulting from a low melting point, high evaporative pressure and a remarkable difference in melting temperature with the other metals, Mg-Ni intermetallic alloy was used instead of Mg, and a slight excess of Mg was used to compensate for

Translated from *Journal of Xi'an Jiao Tong University*, 2008, 42(3) (in Chinese)

Shumin HAN (✉), Yuan LI, Xilin ZHU, Lin HU
School of Environmental and Chemical Engineering, Yanshan University, Qinhuangdao 066004, China
E-mail: hanshm@ysu.edu.cn

Shumin HAN, Zhong ZHANG, Jinhua LI
State Key Laboratory of Metastable Materials Science and Technology, Yanshan University, Qinhuangdao 066004, China

evaporative Mg loss during the melting procedure. The purity of the other metals was more than 99.5%. The ingots were then annealed at 1173 K for 8 h. The chemical composition of the alloy was finally examined by ICP analysis. The prepare ingots were mechanically crushed and ground into fine powder in air. Powders of 200–400 meshes were used for electrochemical testing.

1.2 Structural analysis

The alloy powers under 300 meshes were used for XRD measurement. The XRD data were collected on a D/max-2500/PC Diffractometer using Cu Kα radiation, with a range 10–80° of 2θ and a step interval of 0.02° and a count time of 1 s per step. The data was analyzed using Jade 5.0 software. The morphology was obtained by SEM, and the chemical composition for each phase was analyzed by EDX.

1.3 Measurements for electrochemical properties

A testing electrode was prepared by cold pressing a mixture of 0.15 g alloy powders and 0.75 g carbonyl nickel powders into a pellet of 10 mm in diameter and 1 mm in thickness under 15 MPa. The electrochemical measurements were performed in a system consisting of a working electrode (MH), a counter electrode ($Ni(OH)_2$/NiOOH) and 6 mol/L KOH electrolyte. The electrochemical tests were performed on a DC-5 Constant Current Testing Instrument. The electrodes were charged at 72 mA/g for 8–10 h and then discharged at the same current density to a cut-off voltage of 1.0 V. The interval between charge and discharge was 10 min. When the high rate dischargeability (HRD) was measured, capacity at various current densities was recorded. The calculation method for HRD and capacity retention rate was as in our previous report [11].

2 Results and discussion

2.1 Structural analyses

Table 1 shows compositions of the $Ml_{0.88}Mg_{0.12}Ni_{3.0}Mn_{0.10}Co_{0.55}Al_{0.10}$ alloy (Alloy A for brevity, below), including the designing composition and final composition measured by ICP. There is no noticeable difference between these two compositions for each element. It is calculated from Table 1 that the designing formula is $Ml_{0.88}Mg_{0.12}Ni_{3.0}Mn_{0.10}Co_{0.55}Al_{0.10}$, while the final one is $Ml_{0.88}Mg_{0.12}Ni_{2.98}Mn_{0.11}Co_{0.56}Al_{0.11}$. This indicates that uncertainty in composition resulting from Mg eva-poration has been eliminated, and the desired composition can be obtained.

Table 1 Chemical compositions of $Ml_{0.88}Mg_{0.12}Ni_{3.0}Mn_{0.10}Co_{0.55}Al_{0.10}$ alloy(%)

	Ml	Mg	Ni	Mn	Co	Al
Designing composition	35.9	0.852	51.4	1.68	9.47	0.828
Final composition	35.9	0.853	51.1	1.76	9.48	0.858

Figure 1 shows the XRD patterns of Alloy **a** and commercial AB_5-type alloy (Alloy **b** for brevity, below). As analyzed by Jade 5.0, Alloy **a** consists of $CaCu_5$-type, Ce_2Ni_7-type and Pr_5Co_{19}-type phases, while Alloy **b** consists of **a** single $CaCu_5$-type phase.

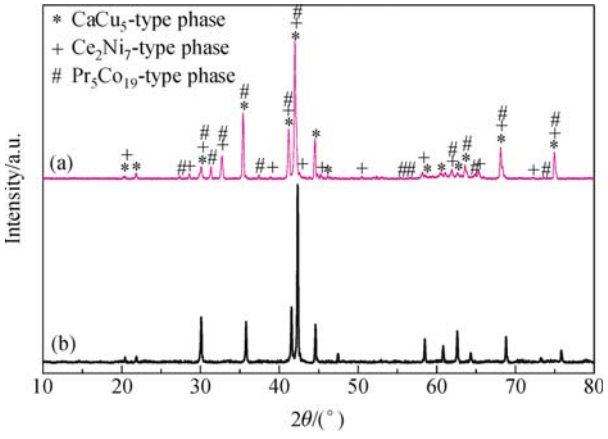

Fig. 1 XRD patterns of $Ml_{0.88}Mg_{0.12}Ni_{3.0}Mn_{0.10}Co_{0.55}Al_{0.10}$ (**a**) and AB_5 alloy (**b**)

The back scattering electron (BSE) image of $Ml_{0.88}Mg_{0.12}Ni_{3.0}Mn_{0.10}Co_{0.55}Al_{0.10}$ is shown in Fig. 2. The light grey, dark grey and black areas are attributed to three different phases, designated as α phase, β phase and γ phase, respectively. EDX analysis shows that they are the Ce_2Ni_7-type, Pr_5Co_{19}-type and $CaCu_5$-type phases, respectively. The Ce_2Ni_7-type phase and Pr_5Co_{19}-type phase distribute continuously and the $CaCu_5$-type phase inserts into the other two phases at small amounts.

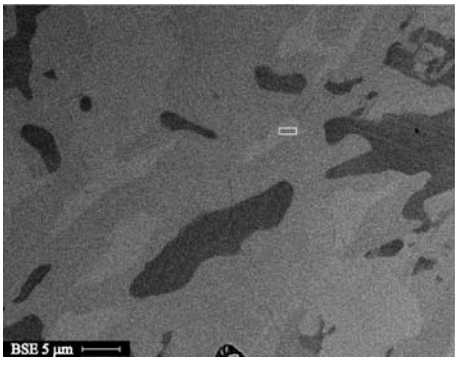

Fig. 2 Back scattering electron image of $Ml_{0.88}Mg_{0.12}Ni_{3.0}Mn_{0.10}Co_{0.55}Al_{0.10}$ alloy

2.2 Electrochemical properties

Figure 3 shows the discharge capacity varying with cycle number. It can be seen that Alloy **a** is completely activated

within 2 charge/discharge cycles and Alloy **b** needs 3 cycles for complete activation. The discharge capacity of Alloy **a** reaches 386 mAh/g, 16.3% higher than that of Alloy **b**.

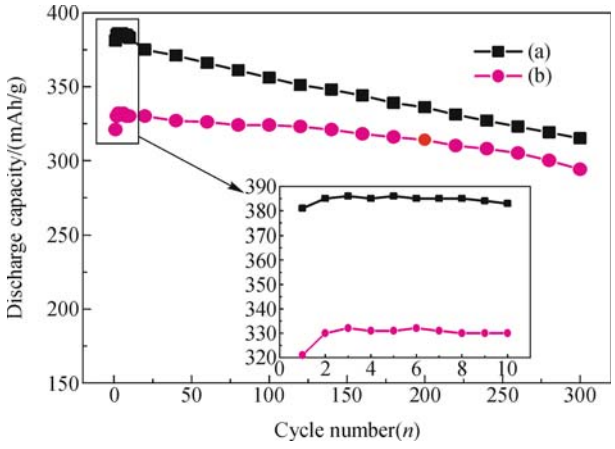

Fig. 3 Capacities varying with cycle numbers for $Ml_{0.88}Mg_{0.12}Ni_{3.0}Mn_{0.10}Co_{0.55}Al_{0.10}$ (**a**) and AB_5 (**b**) alloy electrodes

The good activation property of the Ml-Mg-Ni-based alloy is related to its multi-phase structure, for the multi-phase structure increases boundaries area between phases. When H atoms enter interstices, the lattices are deformed and stress energy is formed. However, the phase boundaries help to reduce lattice deformation and stress energy. Meanwhile, the boundaries provide channels for hydrogen diffusion, so the activation property is improved [13]. From the BSE image of Alloy **a**, the $CaCu_5$-type phase with high catalytic activity inserts into the Ce_2Ni_7-type and Pr_5Co_{19}-type phases with larger hydrogen storage capacity. The $CaCu_5$-type phase works as the catalytic phase for hydriding/dehydriding of the Ce_2Ni_7-type and Pr_5Co_{19}-type phases, while it works as a hydrogen storage phase itself, and thus electrochemical capacity of the electrode is promoted.

However, degradation in the capacity of Alloy **a** is faster that that in Alloy **b**. The discharge capacity for Alloy **a** and **b** is 315 mAh/g and 294 mAh/g, respectively, retaining 81.5% and 89.0% of their maximum discharge capacity, respectively. The faster degradation for Alloy **a** can be explained by serious oxidation and pulverization [11]. During charge/ discharge processing, pulverization happens to alloy particles, enlarging specific areas and thus accelerating oxidation. Meanwhile, Mg is easily oxidized into its hydroxide $Mg(OH)_2$, forming a loose passive layer at surfaces. As a result, the active component for hydrogen storage reduces in content, leading to decreasing hydrogen capacity.

Figure 4 shows the relationship between high rate dischargeability (HRD) and current density for Alloy **a** and **b**. It is noticed that **a** has higher HRD than **b**, and the difference between HRD for the two alloys enhances with increasing discharge current density. When discharge current density is 360 mA/g, HRD is 88% and 84% for Alloy **a** and **b**, respectively, showing **a** 4% difference. While the discharge current density increases to 1800 mA/g, the HRD for Alloy **a** and **b** decreases to 38% and 14%, respectively, or a 24% difference.

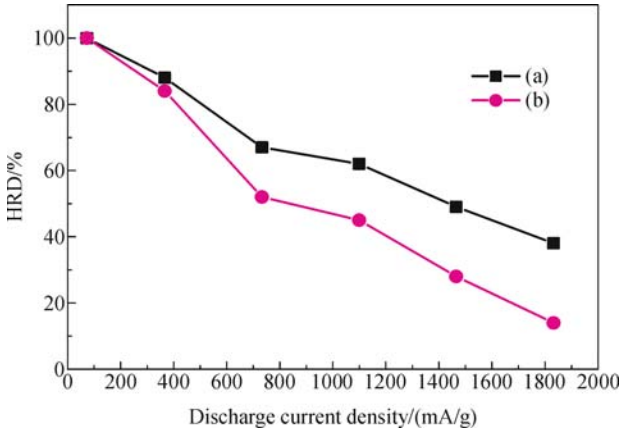

Fig. 4 HRD of $Ml_{0.88}Mg_{0.12}Ni_{3.0}Mn_{0.10}Co_{0.55}Al_{0.10}$ (**a**) and AB_5 (**b**) alloy electrodes

It is generally believed that HRD is mainly controlled by kinetics, including charge-transfer reactions at the surface and hydrogen diffusion in bulk [14]. It can be seen from the BSE image that distribution of inter-inserting phases and boundaries between different phases provide a large specific area and a hydrogen diffusion channel, accelerating electrochemical reactions on the electrodes. The multiphase structure facilitates Alloy A to overcome difficulties in stable hydride and slow hydrogen release, and thus improves HRD for Alloy A.

3 Conclusion

The Ml-Mg-Ni-based $Ml_{0.88}Mg_{0.12}Ni_{3.0}Mn_{0.10}Co_{0.55}Al_{0.10}$ alloy was prepared by inductive melting. The as-prepared alloy consists of $CaCu_5$-type, Ce_2Ni_7-type and Pr_5Co_{19}-type phases. The electrochemical measurements show that discharge capacity of the alloy is as high as 386 mAh/g, 16.3% higher than that of the commercial AB_5-type alloy (332 mAh/g). At discharge current density of 1 100 mA/g, high rate dischargeability reaches 65%, much higher than that of the AB_5-type alloy (45%). After 300 charge/discharge cycles, the capacity of the Ml-Mg-Ni-based alloy decreases to 315 mAh/g, retaining 81.5% of the maximum discharge capacity.

References

1. Pan H G, Ma J X, Wang C S, Chen S A, Wang X H, Chen C P, Wang Q D. Studies on the electrochemical properties of $MlNi_{4.32-x}Co_x$

$Al_{0.7}$ hydride alloy electrodes. Journal of Alloys and Compounds, 1999, 293–295: 648–652

2. Kadir K, Sakai T, Uehara I. Structural investigation and hydrogen capacity of $LaMg_2Ni_9$ and $(Y_{0.65}Ca_{0.35})(Mg_{1.32}Ca_{0.68})Ni_9$ of the AB_2C_9 type structure. Journal of Alloys and Compounds, 2000, 302 (1–2): 112–117
3. Chen J, Takeshita H T, Tanaka H, Kuriyama N, Sakai T, Uehara I, Haruta M. Hydriding properties of $LaNi_3$ and $CaNi_3$ and their substitutes with $PuNi_3$-structure. Journal of Alloys and Compounds, 2000, 302(1–2): 304–313
4. Kohno T, Yoshida H, Kawashima F, Inaba T, Sakai I, Yamamoto M, Kanda M. Hydrogen storage properties of new ternary system alloys: La_2MgNi_9, $La_5Mg_2Ni_{23}$, La_3MgNi_{14}. Journal of Alloys and Compounds, 2000, 311(2): L5–L7
5. Akiba E, Hayakawa H, Kohno T. Crystal structure of novel La-Mg-Ni hydrogen absorbing alloys. Journal of Alloys and Compounds, 2006, 408–412: 280–283
6. Pan H G, Liu Y F, Gao M X, Zhu Y F, Lei Y Q. The structural and electrochemical properties of $La_{0.7}Mg_{0.3}(Ni_{0.85}Co_{0.15})_x$ (x = 3.0–5.0) hydrogen storage alloys. International Journal of Hydrogen Energy, 2003, 28(11): 1219–1228
7. Liu Y F, Pan H G, Gao M X, Li R, Lei Y Q. Influences of Ni addition on the structures and electrochemical properties of $La_{0.7}Mg_{0.3}$-$Ni_{2.65+x}Co_{0.75}Mn_{0.1}$ (x = 0.0–0.5) hydrogen storage alloys. Journal of Alloys and Compounds, 2005, 389(1–2): 281–289
8. Liao B, Lei Y Q, Chen L X, Lu G L, Pan H G, Wang Q D. Effect of Co substitution for Ni on the structural and electrochemical properties of $La_2Mg(Ni_{1-x}Co_x)9$ (x = 0.1–0.5) hydrogen storage electrode alloys. Electrochimica Acta, 2004, 50(4): 1057–1063
9. Liu Y F, Pan H G, Zhu Y F, Li R, Lei Y Q. Influence of Mn content on the structural and electrochemical properties of the $La_{0.7}Mg_{0.3}Ni_{4.25-x}Co_{0.75}Mn_x$ hydrogen storage alloys. Materials Science and Engineering A, 2004, 372(1–2): 163–172
10. Liao B, Lei Y Q, Chen L X, Lu G L, Pan H G, Wang Q D. The effect of Al substitution for Ni on the structure and electrochemical properties of AB_3-type $La_2Mg(Ni_{1-x}Alx)_9$ (x = 0–0.05) alloys. Journal of Alloys and Compounds, 2005, 404–406: 665–668
11. Li M, Han S M, Li Y, Guan W, Mao L R, Hu L. Study on the phase structure and electrochemical properties of $RE_{0.93}Mg_{0.07}Ni_{2.96}$-$Co_{0.60}Mn_{0.37}Al_{0.17}$ hydrogen storage alloy. Electrochimica Acta, 2006, 51(26): 5926–5931
12. Zhang Z, Han S M, Li Y, Jing T F. Electrochemical properties of $Ml_{1-x}Mg_xNi_{3.0}Mn_{0.10}Co_{0.55}Al_{0.10}$ (x = 0.05–0.30) hydrogen storage alloys. Journal of Alloys and Compounds, 2007, 431(1–2): 208–211
13. Zhang Y H, Dong X P, Wang G Q, Ren J Y, Guo S H, Wang X L. Microstructures and Electrochemical Performances of La_2Mg-$(Ni_{0.85}Co_{0.15})_9Cr_x$ (x = 0–0.2) Electrode Alloys Prepared by Casting and Rapid Quenching. Rare metal Materials and Engineering, 2006, 35(6): 876–879 (in Chinese)
14. Iwakura C, Oura T, Inoue H, Matsuoka M. Effects of substitution with foreign metals on the crystallographic, thermodynamic and electrochemical properties of AB_5-type hydrogen storage alloys. Electrochimica Acta, 1996, 41(1): 117–121